CHM/REP1 Transcript Expression and Loss of Visual Function in Patients Affected by Choroideremia

Valentina Di Iorio,[1] Gabriella Esposito,[2,3] Francesca De Falco,[2,3] Rosa Boccia,[1] Tiziana Fioretti,[4] Raffaella Colucci,[1] Giuseppe De Rosa,[1] Paolo Melillo,[1] Francesco Salvatore,[3,4] Francesca Simonelli,[1] and Francesco Testa[1]

[1]Eye Clinic, Multidisciplinary Department of Medical, Surgical and Dental Sciences, University of Campania Luigi Vanvitelli, Naples, Italy
[2]Department of Molecular Medicine and Medical Biotechnologies, University of Naples Federico II, Naples, Italy
[3]CEINGE-Biotecnologie Avanzate s.c.a r.l., Naples, Italy
[4]IRCCS SDN, Naples, Italy

Correspondence: Francesca Simonelli, Eye Clinic, Multidisciplinary Department of Medical, Surgical and Dental Sciences, University of Campania Luigi Vanvitelli, Via S. Pansini, 5, Naples 80131, Italy; francesca.simonelli@unicampania.it.

VDI and GE contributed equally to the work presented here and should therefore be regarded as equivalent authors.

Submitted: August 12, 2018
Accepted: January 22, 2019

Citation: Di Iorio V, Esposito G, De Falco F, et al. *CHM/REP1* transcript expression and loss of visual function in patients affected by choroideremia. *Invest Ophthalmol Vis Sci*. 2019;60:1547–1555. https://doi.org/10.1167/iovs.18-25501

Purpose. To evaluate the disease progression in patients with clinical and genetic diagnoses of choroideremia during a long-term follow-up and to investigate the relationship between pathogenic variants in the *CHM/REP1* gene and disease phenotypes.

Methods. We performed a retrospective longitudinal study on 51 affected men by reviewing medical charts at baseline and follow-up visits to extract the following ocular findings: best-corrected visual acuity, Goldmann visual field, optical coherence tomography, microperimetry. Data obtained from the analysis of DNA and mRNA were reevaluated for genetic classification of patients.

Results. The longitudinal analysis showed a significant ($P < 0.001$) worsening of best-corrected visual acuity with a mean rate of 0.011 logMar per year before 50 years and 0.025 logMar per year after 50 years. Similarly, V4e Goldmann visual field area significantly ($P \leq 0.01$) decreased at a mean rate of 2.7% per year before 40 years and 5.7% after 40 years. Moreover, we observed a significant ($P < 0.05$) decrease of macular sensitivity with a mean rate of 5.0% per year and a decrease of mean macular thickness with a mean rate of 0.8% per year. We classified our patients into two groups according to the expression of the *CHM/REP1* gene transcript and observed that mutations leading to mRNA absence are associated with an earlier best-corrected visual acuity and Goldmann visual field loss.

Conclusions. Our analysis of morphological and functional parameters in choroideremia patients showed a slow disease progression, particularly in the first decades of life. Overall, reevaluation of clinical and molecular data suggests exploring the genotype–phenotype relationship based on *CHM/REP1* transcript expression.

Keywords: choroideremia, visual field, visual acuity, genotype-phenotype correlation, longitudinal study

Choroideremia (CHM) is an inherited eye disease characterized by progressive and diffuse degeneration of the retinal pigment epithelium (RPE) and photoreceptor layers followed by choroid deterioration. Its prevalence is estimated as 1:50,000 males in people of European descent, with the highest prevalence in Northern Finland.[1,2] In affected males, the onset of disease is characterized by night blindness followed by the gradual constriction of peripheral vision and later by a loss of central visual acuity, with progressive structural changes detectable also when central visual function is preserved.[3] Fundus examination shows scalloped areas of confluent loss of RPE and choriocapillaris; underlying photoreceptors in these areas degenerate as well. Optical coherence tomography (OCT) imaging confirms atrophy of RPE and choriocapillaris with overlying preservation of retinal thickness albeit with anomalous lamination. Full-field electroretinogram (ERG) reveals distinct dysfunction in rod and cone photoreceptors. Usually changes in the fundus appearance closely match areas of peripheral Goldmann visual field (GVF) loss that manifests as ring scotoma.

The disorder is caused by loss-of-function mutations in the *CHM/REP1* gene (HGNC:1940), on chromosome X, which encodes the ubiquitous Rab escort protein 1 (REP1; NP_000381.1), also known as component A of Rab geranylgeranyl-transferase,[4] which is involved in intracellular vesicle trafficking and recycling. A similar function is exerted in tissues other than the retina by the Rab escort protein 2 (NP_001812.2), which is expressed by the *CHML* gene (HGNC:1941), on chromosome 1. Functional studies showed that efficiency of the REP1-mediated prenylation is higher than Rab escort protein 2,[5] supporting the evidence that Rab escort protein 2 alone is not able to replace the total loss of *CHM/REP1* function in CHM patients. Despite the characterization of the genetic basis of the disease, until now no studies have established the correlation between mechanisms of vision loss associated with CHM and the genotypic pattern. A study by Freund et al.[6] supported the fact that the rare *CHM/REP1*

pathogenic missense variants do not seem to cause a milder phenotype when compared with whole gene deletions or to the most common type of *CHM/REP1* pathogenic variants (i.e., those leading to putative truncated proteins), thereby indicating that there are no genotype–phenotype correlations in males affected by CHM.

To date, few reports scanned the longitudinal study of the natural history of CHM. Some studies investigated the clinical evolution of the disease in terms of visual acuity[7,8]; other studies reported both clinical and genetic analyses, focusing on visual impairment and visual field constriction[6] and on electrophysiological variability.[9] Because clinical studies evaluating the effect of experimental treatments for CHM are underway, the accurate description of the disease course in genetically characterized CHM patients is warranted.[10,11] Knowledge regarding CHM natural evolution and any genotype correlation could drive the selection of subjects to be enrolled in clinical trials as well as the outcomes of experimental therapy on disease progression. To this end, the present study aims to track disease progression during a long-term follow-up period in a cohort of patients with complete clinical and molecular diagnoses of CHM and to unveil any new phenotype–genotype correlations.

Material and Methods

Patients

A total of 60 men affected by CHM were examined in the Referral Center of Hereditary Retinal Dystrophies of the University of Campania "Luigi Vanvitelli" (baseline examination from January 1, 1994 to December 31, 2014). The affected men ($n = 9$) who tested negative for a *CHM/REP1* gene mutation have not been further considered for the purpose of the present study. Ophthalmological examination included the following tests: best-corrected visual acuity (BCVA) using the Snellen visual chart, slit-lamp biomicroscopy of anterior segment and fundus examination, fundus imaging, GVF, microperimetry (MP1), OCT, and ERG. Longitudinal ERG data were not included because ERG responses were below the noise level at the first visit in most patients.

Digital fundus photographies were taken by a trained ophthalmic photographer using a high-resolution digital camera (Canon EOS D30, Rochester, NY, USA) attached to a 45° fundus camera (Canon CR6-45NM). The fundus alterations were evaluated by fundus images according to Krill's classification[12] in the following three stages: (1) initial stage, characterized by abnormal pigmentary stripping and fine atrophy of the RPE, mild atrophy of the larger choroidal vessels, and focal areas of choriocapillary atrophy; (2) second stage in which there may be a spread of the choroidal atrophy from the equatorial regions inward and from the optic disc outward; and (3) last stage in which there are additional widespread chorioretinal atrophy, attenuation of retinal vessels, and mild optic disc pallor.

GVF was measured by moving the III4e and V4e stimulus targets on a calibrated standard Goldmann perimeter by the same experienced ophthalmic technician and analyzed as previously published.[13] In particular, the average radius of the central GVF was measured at 12 meridians (the main four meridians and eight equally spaced intermediate meridians, two in each quadrant) to obtain the estimated area, calculated simply as πr^2 and expressed in square degrees ($^{\circ 2}$). Any peripheral island, when present, was not included in the central GVF measurement, and any scotomatous area, except a physiological blindspot, was measured with the same method and subtracted from the total area.

Full-field ERG was recorded by corneal contact lens electrodes with a Ganzfeld stimulator (Roland Consult, Brandenburg an der Havel, Germany) using the standard protocol proposed by the International Society for Clinical Electrophysiology of Vision.[14]

Spectral-domain OCT (Cirrus HD-OCT; Carl Zeiss, Dublin, CA, USA), available since 2009, was performed according to the following protocol: the acquisition protocol comprised a five-line raster scan and a macular cube scan pattern (512 × 128 pixels) in which a 6 × 6 mm region of the retina was scanned within a scan time of 2.4 seconds. The retinal thickness analysis protocol provided with the instrument software was used to calculate the mean macular thickness (MMT).

MP1 was performed by an automatic fundus-related perimeter (MP1 Microperimeter, Nidek Technologies, Padova, Italy), available since 2008. To evaluate macular sensitivity (MS) the following parameters were used: a fixation target of 2° in a diameter consisting of a red ring; a white, monochromatic background with a luminance of 1.27 cd/m^2; a Goldmann V–size stimulus with a projection time of 200 milliseconds; and a predefined automatic macular test pattern covering 6° centered on the gravitational center of all the fixation points with 43 stimuli.

The study adhered to the tenets of the Declaration of Helsinki and was approved by Ethics Committee of the Second University of Napoli (now named University of Campania Luigi Vanvitelli [Naples, Italy]). Moreover, each patient gave written informed consent for involvement in this retrospective chart-review study.

Molecular Analysis

DNA and total RNA were extracted from peripheral blood leukocytes according to standard methods. Exons 1 to 15 of the *CHM* gene were amplified by PCR and analyzed as previously described.[15] We also extended the molecular study by analyzing the effect of pathogenic variants on *CHM/REP1* mRNA in 42 of our patients. To this aim, we isolated total RNA and carried out RT-PCR to detect the *CHM/REP1* transcript; cDNA amplicons, if obtained, were analyzed by sequencing.[15] Mutation numbering was based on the genomic and mRNA reference sequences of *CHM/REP1* (GenBank #NG_009874.2, NM_000390.3; NP_000381.1).

Statistics

Continuous data are expressed as mean ± standard error of the mean. Repeated-measure longitudinal regression, estimated by a generalized estimating equations, was used to estimate the mean rate of change for each outcome measure. Generalized estimating equations were adopted because this method could deal with the intereye correlation (i.e., between the two eyes of the same person at a given visit) and longitudinal correlation (i.e., between values of the same eye followed over time) by adopting an appropriate covariance structure, as previously described.[16–18] The method has been previously applied both to investigate treatment effect in ophthalmological studies[19,20] and to evaluate the natural history in inherited retinal diseases.[21–25] BCVA were converted to logMAR and all the other measures (i.e., GVF area, MS, MMT) were log transformed. Moreover, following evidence from previous studies,[6,8] for BCVA and GVF area, two-phase models with a different age cut-off (i.e., 20, 30, 40, or 50 years) were fitted to find eventual changes in the progression rate, and the model with the best goodness of fit (i.e., the minimum value of the corrected quasi likelihood under independence model

Investigative Ophthalmology & Visual Science

criterion) was selected. A repeated-measure longitudinal regression model was fitted to explore the correlation between values of the right and the left eyes. A Kaplan-Meier survival analysis was performed to show the age distribution for blindness, based on BCVA and GVF, and the distributions were compared with a log rank (Mantel-Cox) test. We adopted the following failure criteria for blindness, as indicated by the *International Classification of Diseases* (version 2016)[26]: BCVA worse than 20/400 in the better eye and III4e GVF area in the better eye no greater than 314°^{2} (i.e., corresponding to an equivalent radius of 10°). Finally, to explore any possible genotype–phenotype correlation, we fitted the regression models including as variables patients' age and effect of pathogenic sequence variants on the *CHM/REP1* transcript expression and their interaction. In these analyses, we included only one proband for each family (i.e., the first diagnosed patient, which has, in Table 1, the lowest ID number among the family components), and we excluded the patients for whom RNA analysis was not available.

Results

A total of 51 patients (mean age of 38.0 ± 2.2 years old at baseline) from 36 families with a disease-causing mutation in *CHM* were involved in this clinical study. The most relevant clinical features at the study baseline and molecular genetic findings for each patient are reported in Table 1. In the study cohort, mean BCVA (at first visit) was 0.54 ± 0.13 logMAR in the right eyes and 0.62 ± 0.13 logMAR in the left eyes. Of the patients, 2 showed unilateral cataract and 12 showed a bilateral posterior subcapsular cataract. One subject was pseudophakic in both eyes, and one subject was pseudophakic in one eye.

A typical CHM ocular fundus was observed in all patients. With regard to fundus changes, at the study baseline, 8 patients (mean age 30.7 years) showed a first stage of retinal alteration characterized by abnormal pigmentary stripping and fine atrophy of the RPE, mild atrophy of the larger choroidal vessels, and focal areas of choriocapillary atrophy; 22 patients with a second stage of disease (mean age 33.6 years) presented with choroidal atrophy from the equatorial regions inward and from the optic disc outward; finally, 21 patients (mean age 45.4 years) showed additional widespread chorioretinal atrophy, attenuation of retinal vessels, and mild optic disc pallor according to the third stage of fundus abnormalities according to Krill's classification. Moreover, at the study baseline, GVF, when evaluable ($n = 32$) was constricted (mean area with the V4e stimulus target: 4400 ± 778°^{2} in the right eyes; 4320 ± 776°^{2} in the left eyes).

OCT scans showed, on average, a MMT of 250.5 ± 17.0 μm in the right eyes and 251.8 ± 20.1 μm in the left eyes. Microperimetric findings showed a markedly reduced MS (mean 6.2 ± 5.7 decibels in the right eyes; mean: 5.0 ± 3.6 decibels in the left eyes). Dark-adapted ERG responses were below the noise level in all but 3 patients (1 with a markedly reduced response and 2 with subnormal traces), whereas light-adapted ERG responses were detectable in 14 patients, even if with a marked reduction of amplitude in all but 3 patients (with subnormal or normal responses).

Figure 1 reports the mean annual rates of disease progression in terms of BCVA and GVF area in the patients with a mean follow-up of 9 years. According to a one-phase model, BCVA worsened with a mean rate of 0.021 logMAR (about 1 ETDRS letter) per year ($P < 0.001$). Moreover, we observed significant decreases in GVF area in response to III4e stimulus size with a mean exponential rate of 4.8% per year ($P < 0.001$) and in response to V4e stimulus size with a mean exponential rate of 4.5% per year ($P < 0.001$). However, the two-phase models better fit the BCVA and GVF data than the one-phase models. In particular, the cut-off for loss of BCVA was 50 years of age, which defined a break in a biphasic model of decline: BCVA declined at a mean rate of 0.011 logMAR per year before 50 years of age and 0.025 logMAR per year after age 50. The critical age for loss of the GVF was 40 years, with the III4e area decreasing at a mean rate of 2.9% per year before 40 years and 8.8% per year after 40 years, and with the V4e area decreasing at a mean rate of 2.7% per year before 40 years and 5.7% per year after 40 years.

Table 2 reports the mean annual rates of MS and MMT, showing a significant decrease in MS with a mean exponential rate of 5.0% per year ($P < 0.001$) and a significant thinning of the MMT with a mean exponential rate of 0.8% per year ($P = 0.017$).

Finally, there was a strong and significant intereye correlation both for BCVA ($\beta = 0.910$; 95% confidence interval [CI] = 0.823–0.996; $P < 0.001$) and for GVF area (stimulus size III4e: $\beta = 1.024$; 95% CI = 0.979–1.070; $P < 0.001$; stimulus size V4e: $\beta = 0.846$; 95% CI = 0.802–0.890; $P < 0.001$), as shown also in Figure 2.

Survival analysis for blindness, reported in Figure 3, shows that the development of blindness was driven primarily by GVF loss: the survival curve based on GVF no greater than 10° (median age 42.8 years; 95% CI = 40.2–45.4 years) is significantly shifted ($P < 0.001$) to younger ages when compared with a survival curve based on a visual acuity of 20/400 or less (median age 63.2 years; 95% CI = 53.7–72.7 years).

Genotyping was carried out by genomic DNA analysis, and *CHM/REP1* pathogenic variants were identified in all 51 patients (Table 1). The genotype of 33 patients has been already reported[15]; among the genomic variants identified in the remaining 18 patients and here reported for the first time, we found two novel pathogenic alleles, that is, the splicing variant c.1166+1G>C and the macrodeletion c.1-?_1510+?del that removes exons 1 to 12 of *CHM/REP1*.

For 42 of our patients, molecular analysis was further performed by analyzing total RNA extracted from leukocytes and, based on the effect of pathogenic sequence variants on the *CHM/REP1* mRNA expression, we recognized two groups of patients. In particular, the first group (group P, transcript present) included 35 patients (from 23 independent families) with mutations that did not impair the *CHM/REP1* gene transcription; indeed, in these patients, the mutated mRNA was detected. The second group (group A, transcript absent) included seven patients (four families) who completely lacked the *CHM/REP1* transcript (see Table 1).

We compared the two groups by fitting regression models, reported in Table 3, only on one proband for each family. With regard to BCVA, we observed a significantly ($P < 0.05$) different behavior; in particular, as shown in Figure 4, BCVA in group P worsened at a rate of 0.039 logMAR per year starting at −0.889 logMAR, whereas BCVA in group A started with a significantly worse value when compared with group P ($P = 0.003$), but it did not significantly ($P > 0.05$) decline with age. Similar to BCVA, the patient group A, when compared with group P, showed a significantly ($P < 0.05$) earlier GVF area loss (using both V4e and III4e stimulus target sizes), without significant progression with age ($P > 0.05$). Consistently, a significantly ($P < 0.05$) slower progression rate in patient group A when compared with group P was observed. A similar trend was observed for MS, but the differences are not statistically significant ($P > 0.05$). Finally, no significant differences ($P > 0.10$) between the two groups were observed in the reduction of MMT.

Investigative Ophthalmology & Visual Science

Table 1. Main Clinical and Genetic Features in Choroideremia Patients

			BCVA (logMAR)		Lens Status		Fundus*	GVF V4e Area (°²)		ERG (Both Eyes)			
ID	Fam. ID	Age, y	RE	LE	RE	LE	Both Eyes	RE	LE	Dark Adapted 0.01	Light Adapted 3.0	*CHM* Pathogenic Variant (NM_000390.3; NP_000381.1)†	mRNA Expression
1	1	27	0.22	0.08	cl	c	2	6326	8252	bnl	bnl	c.1520A>G (p.His507Arg)	P
2	1	19	0.16	0.16	cl	cl	3	12885	8797	bnl	mr	c.1520A>G (p.His507Arg)	P
3	2	57	2.8	2.8	c	c	3	n/a	n/a	bnl	bnl	c.50-?_189+?del	P
4	3	30	0.52	0.92	c	cl	3	207	n.p.	bnl	mr	c.820-2A>G	P
5	4	30	0.02	0.02	cl	cl	3	5487	6708	bnl	bnl	c.315_318del (p.Ser105Argfs)	P
6	5	11	0	0	cl	cl	2	8700	9289	bnl	mr	c.808C>T (p.Arg270*)	n/a
7	6	63	2.8	2.7	p	p	3	n/a	n/a	bnl	bnl	c.808C>T (p.Arg270*)	n/a
8	7	21	0.02	0	cl	cl	2	n/a	n/a	bnl	mr	c.940+1G>T	P
9	8	43	1	0.36	cl	cl	3	n/a	n/a	bnl	bnl	c.49+5C>T	n/a
10	9	36	0	0	c	c	2	n/a	n/a	bnl	bnl	c.1414-?_1510+?del	A
11	9	45	−0.08	0	cl	cl	1	n/a	n/a	bnl	mr	c.1414-?_1510+?del	A
12	9	46	−0.04	−0.04	cl	cl	1	n/a	n/a	bnl	bnl	c.1414-?_1510+?del	A
13	10	33	1.52	0.16	cl	cl	2	n/a	n/a	bnl	bnl	c.1-?_*3450+?del	A
14	11	43	0.1	1	cl	cl	2	143	134	bnl	bnl	c.757C>T (p.Arg253*)	P
15	12	14	−0.04	−0.04	cl	cl	1	73	79	bnl	bnl	c.1651delTACTT	n/a
16	13	45	0.06	0.52	cl	cl	3	7880	8305	bnl	mr	c.969T>A (p.Tyr323*)	P
17	13	58	0.16	0.1	cl	cl	3	252	163	bnl	bnl	c.969T>A (p.Tyr323*)	P
18	15	22	0	0	cl	cl	2	8427	9303	bnl	bnl	**c.1166+1G>C**	P
19	16	65	1.3	1.3	c	c	3	8481	9303	bnl	bnl	c.1218C>A (p.Cys406*)	P
20	17	41	0.16	1.3	cl	cl	3	35	165	bnl	bnl	c.652_654del (p.Ser218Lysfs)	P
21	18	41	0.3	0.7	cl	cl	3	27	66	bnl	bnl	c.877C>T (p.Arg293*)	P
22	19	42	0.2	0.08	cl	cl	3	1056	524	bnl	bnl	c.116+1G>T	P
23	20	11	0	0	cl	cl	1	569	723	bnl	bnl	c.116+1G>T	P
24	14	50	2.7	2.8	c	c	1	n/a	n/a	bnl	s	c.315_318del (p.Ser105Argfs)	P
25	20	20	0	0	cl	cl	2	10920	11786	bnl	bnl	c.116+1G>T	P
26	21	52	0.52	0	c	c	3	252	218	bnl	bnl	c.941-2A>G	P
27	22	7	0.02	0.02	cl	cl	2	7906	7088	bnl	bnl	c.580_581ins (p.Asp184Glufs)	n/a
28	23	36	0.06	0.06	c	c	2	11263	12028	s	s	**c.1-?_1510+?del**	A
29	24	32	0.1	0.3	cl	cl	3	n/a	n/a	bnl	bnl	c.525_526del (p.Glu177Lysfs)	P
30	25	33	2.1	2.7	cl	cl	3	n/a	n/a	bnl	bnl	c.969T>A (p.Tyr323*)	P
31	26	60	−0.08	0.06	cl	cl	2	177	218	bnl	mr	c.1350-1G>A	P
32	27	55	2.7	2.7	c	c	3	n/a	n/a	bnl	bnl	c.1310_1313del (p.Ser437Tyrfs)	P
33	9	17	0	0	cl	cl	1	n/a	n/a	s	n	c.1414-?_1510+?del	A
34	28	34	0.3	0.7	c	c	3	25	50	bnl	bnl	c.(?_49+1)_(1609+1_1610_1)del	n/a
35	29	37	0.3	0.12	cl	cl	2	9999	10967	bnl	mr	c.1029delG (p.Met343Ilefs)	P
36	29	43	0.26	0.26	cl	cl	3	210	167	bnl	bnl	c.1029delG (p.Met343Ilefs)	P
37	30	45	0.4	0.7	cl	cl	2	5498	5027	bnl	bnl	c.799C>T, (p.Arg267*)	P
38	30	47	0.16	0.4	cl	cl	2	20	79	bnl	bnl	c.799C>T, (p.Arg267*)	P
39	31	14	0	0	cl	cl	2	9403	7815	mr	mr	c.969T>A (p.Tyr323*)	P
40	18	68	0.08	0.08	cl	cl	2	n/a	n/a	bnl	bnl	c.877C>T (p.Arg293*)	P
41	18	29	0.08	0.22	cl	cl	2	n/a	n/a	bnl	mr	c.877C>T (p.Arg293*)	P
42	32	58	0.16	0.4	c	c	3	n/a	n/a	bnl	bnl	c.1245-?_1962+?del* (p.Cys416*)	P
43	33	31	0.06	0	cl	cl	1	10312	7815	bnl	mr	c.580_581ins (p.Asp184Glufs)	n/a
44	21	48	0.46	0.26	cl	cl	2	n/a	n/a	bnl	bnl	c. 941- 2A>G (p.Val274Aspfs)	P
45	36	19	0.7	1	cl	cl	2	322	335	bnl	bnl	c.1-?_*3450+?del	A
46	13	67	2.8	2.8	cl	p	3	n/a	n/a	bnl	bnl	c.969T>A (p.Tyr323*)	P
47	32	40	0.16	0.06	cl	cl	2	6048	2574	bnl	bnl	c.1245-?_1962+?del* (p.Cys416*)	P
48	32	36	0.02	1.22	c	c	2	2097	3318	bnl	bnl	c.1245-?_1962+?del* (p.Cys416*)	P
49	34	43	2.8	2.8	c	c	3	n/a	n/a	bnl	bnl	c.703-?_941+?del* (p.Lys234Aspfs)	n/a
50	35	44	0.1	0.1	cl	cl	2	653	715	bnl	bnl	c.1245-?_1413+? (p.Ile416Phefs)	n/a
51	32	31	0	0	c	c	1	4388	3352	bnl	bnl	c.1245-?_1962+?del* (p.Cys416*)	P

cl, clear lens; c, cataract; p, pseudophakia; Fam., family; RE, right eye; LE, left eye; n.p., not performable; n/a, not available; bnl, below noise level; mr, markedly reduced; s, subnormal; n, normal; P, present; A, absent.

* Classification according to Krill and Berger: 1 = abnormal pigmentary stripping and fine atrophy of the retinal pigment epithelium, mild atrophy of the larger choroidal vessels and focal areas of choriocapillary atrophy, 2 = spread of the choroidal atrophy from the equatorial regions inward and from the optic disc outward, 3 = widespread chorioretinal atrophy, attenuation of retinal vessels, and mild optic disc pallor.

† Novel CHM pathogenic variants in bold.

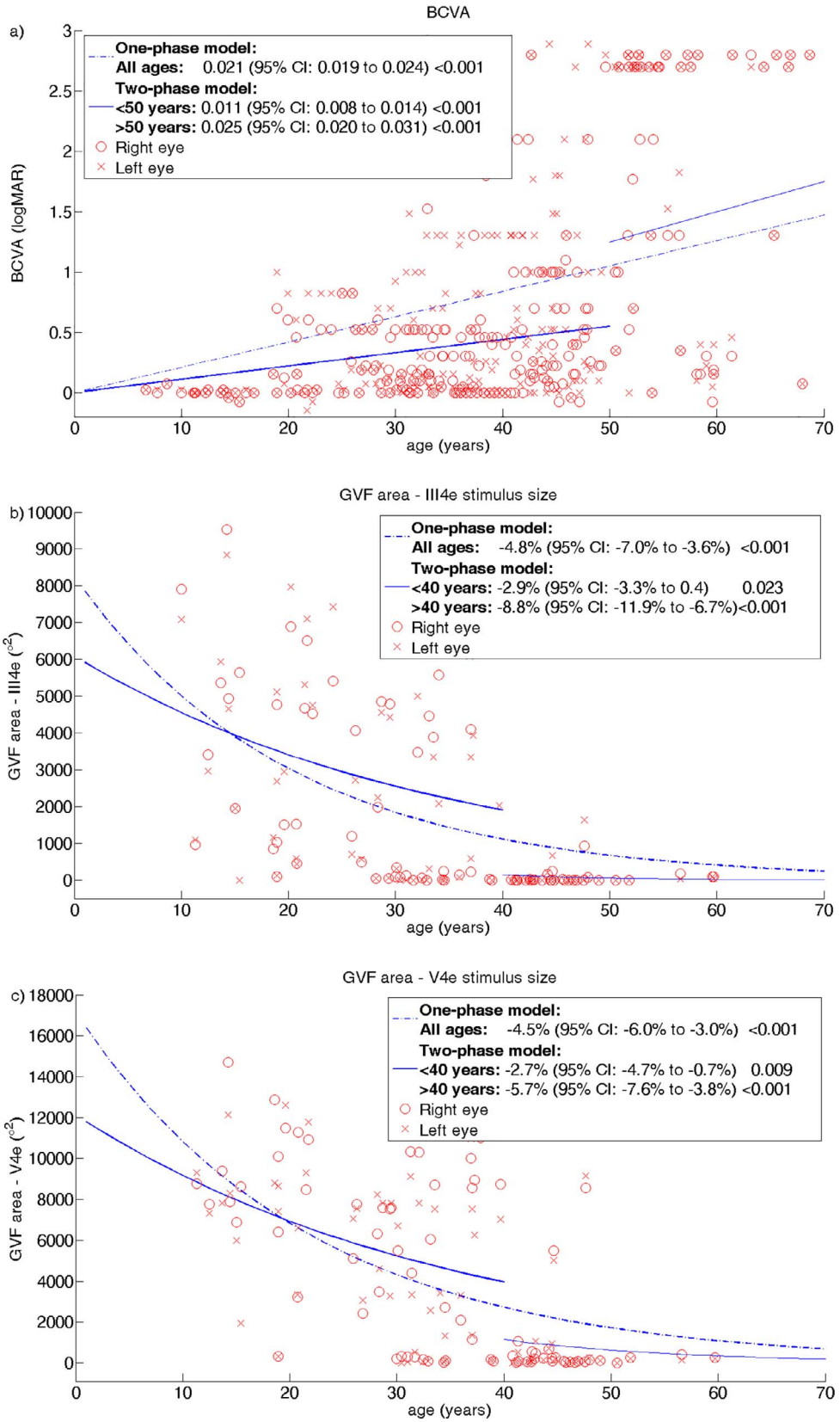

Figure 1. Mean annual progression rate of BCVA (**a**) and GVF area with III4e (**b**) and V4e (**c**) stimulus size in CHM patients. For each model, the mean annual rate (95% CI) with *P* value is reported.

Table 2. Annual Rate of Progression of Macular Sensitivity and Mean Macular Thickness in Choroideremia Patients

Feature	Mean Follow-Up (Patients)	Mean Exponential Annual Rate (95% Confidence Interval)	*P* Value
Macular sensitivity, dB	2.4 years (17)	−5.0% (−6.2% to −3.7%)	**<0.001**
Mean macular thickness, μm	2.7 years (27)	−0.8% (−1.4% to −0.1%)	**0.017**

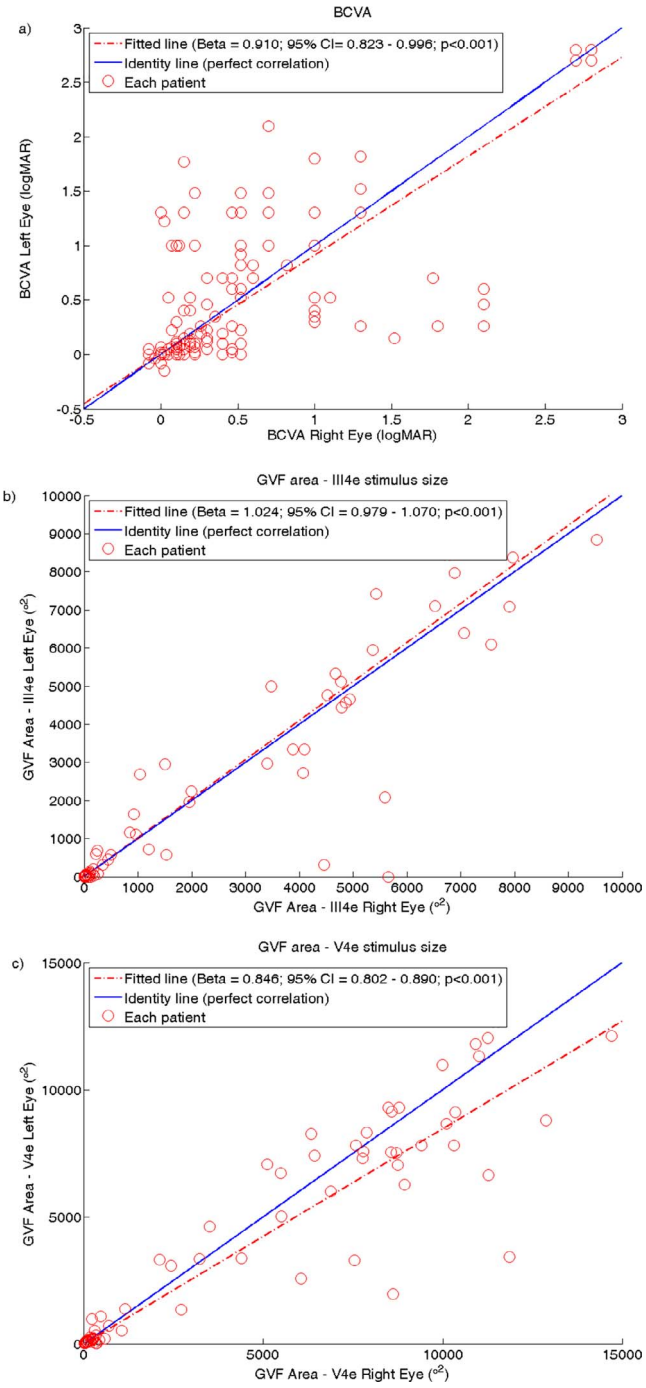

Figure 2. The intereye correlation of BCVA (**a**) and GVF area with III4e (**b**) and V4e (**c**) stimulus size in CHM patients. For each model, the beta (95% CI) with *P* value is reported.

Discussion

The current study proposed a longitudinal analysis in a relatively large cohort of molecularly defined CHM patients, investigating changes in BCVA, GVF, OCT, and MP1.

A few previous studies described the BCVA change in CHM small case series by showing linear progression rates ranging from 0.0072 to 0.018 logMAR per year.[6,8,27] Moreover, because the first studies showed a preservation of the fovea until late in the course of CHM, recently Coussa et al.[8] proposed a two-phase model to describe the progressive loss of BCVA. For this reason, we also adopted a two-phase model on our data and showed that the critical age for decline of BCVA in our cohort was 50 years of age, with a worsening at a mean rate of 0.011 logMAR per year before 50 years of age and 0.025 logMAR per year after age 50. These findings on BCVA appear to be in agreement with a BCVA loss rate of 0.021 logMAR per year after age 50, as described by Coussa et al.[8] and with a quicker worsening of visual acuity after age 40, as described by Freund et al.[6] and Aleman et al.[27] Regarding visual field loss, the critical age in our patients was 40 years; in particular, using the III4e stimulus target, the GVF area decreased at a mean rate of 2.9% per year before 40 years and 8.8% per year after 40 years. On the contrary, Freund et al.[6] proposed a biphasic pattern of the GVF, reporting that the critical age using the III4e stimulus target is 20 years. However, the loss of GVF reported by Freund et al.[6] in patients younger than 20 years of age was conditioned by high variability of the GVF and no statistical significance, as noted by the authors. Moreover, we estimated CHM disease progression in terms of MS and MMT, 5.0% per year and 0.8% per year, respectively, suggesting the usefulness of MP1 and OCT in the follow-up of CHM. In this regard, our findings are consistent with the cross-section estimates of the annual reduction of foveal thickness recently reported by Aleman et

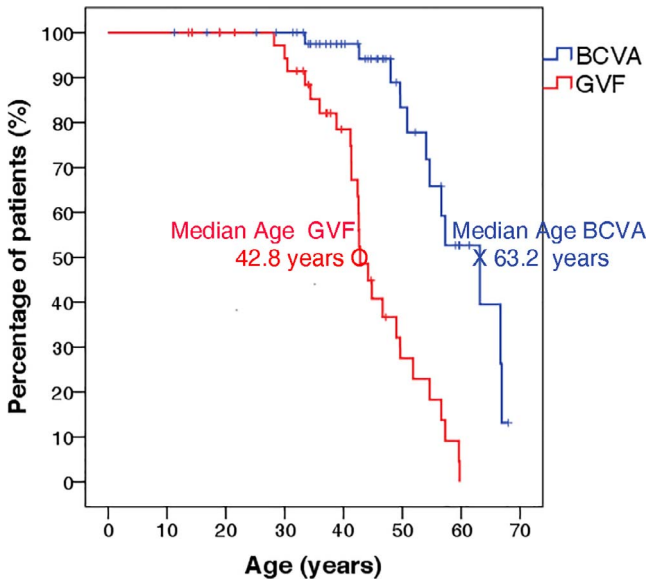

Figure 3. Kaplan-Meier survival curves for BCVA (≤20/400) and GVF area with III4e stimulus size (<314°²) in the better eye in CHM patients.

Table 3. Regression Models to Compare the Disease Progression in Choroideremia Patients According to the *CHM/REP1* mRNA Expression

Dependent Variable	Covariate	Group P, Present Transcript β (95% CI)	*P* Value	Group A, Absent Transcript β (95% CI)	*P* Value	Group A Compared With Group P β (95% CI)	*P* Value
Best-corrected visual acuity, logMAR	Intercept	−0.889 (−1.524 to −0.253)	0.006	0.777 (−0.129 to 1.682)	0.093	**1.665 (0.559 to 2.771)**	**0.003**
	Age	0.039 (0.027 to 0.052)	<0.001	−0.006 (−0.042 to 0.029)	0.732	**−0.046 (−0.083 to 0.008)**	**0.018**
Log visual field area V4e, °^{2}	Intercept	11.037 (10.11 to 11.96)	<0.001	8.732 (7.828 to 9.637)	<0.001	**−2.305 (−3.598 to −1.011)**	**<0.001**
	Age	−0.089 (−0.127 to −0.05)	<0.001	−0.016 (−0.056 to 0.025)	0.445	**0.073 (0.017 to 0.129)**	**0.010**
Log visual field area III4e, °^{2}	Intercept	11.047 (8.72 to 13.374)	<0.001	8.021 (7.082 to 8.999)	<0.001	**−3.026 (−5.55 to −0.502)**	**0.019**
	Age	−0.125 (−0.228 to −0.023)	0.016	−0.013 (−0.059 to 0.032)	0.581	**0.113 (0.001 to 0.224)**	**0.048**
Log macular sensitivity, dB	Intercept	7.183 (4.8 to 9.565)	<0.001	3.785 (0.589 to 7.000)	0.020	−3.388 (−7.381 to 0.606)	0.096
	Age	−0.207 (−0.316 to −0.099)	<0.001	−0.063 (−0.161 to 0.034)	0.204	0.144 (−0.002 to 0.29)	0.053
Log mean macular thickness, µm	Intercept	6.315 (5.929 to 6.7)	<0.001	7.459 (5.910 to 9.008)	<0.001	1.144 (−0.452 to 2.741)	0.160
	Age	−0.023 (−0.032 to −0.013)	<0.001	−0.054 (−0.105 to −0.004)	<0.001	−0.032 (−0.083 to 0.02)	0.227

Bolded values are statistically significant differences.

al.[27] of about 2 µm per year. Finally, we observed a significant intereye correlation for BCVA and GVF, consistent with all previous studies.[6,8,27] The strong intereye correlation at a single time point could enable treating one eye and using the other one as a nonmanipulated control in open-label clinical trials, for example, to investigate gene therapy.

Although some clinical studies[6,9] also evaluated the patients' genotype, no apparent genotype–phenotype correlations have so far emerged for CHM. These studies correlated eye-specific clinical findings to the predicted effect of a DNA variant on the residual function of REP1. However, according to the molecular basis of CHM, most mutations cause absent or strongly deficient REP1 protein expression.[28] Therefore, phenotype–genotype correlation should not depend on the protein dysfunction, but on others, to date unconsidered, mechanisms. Thus, in our patients, we considered *CHM/REP1* gene expression a possible determinant of the CHM phenotype variability. On this basis, we recognize two different groups of patients, that is, patients who express (group P, mRNA present) and patients who do not express (group A, mRNA absent) the *CHM/REP1* mRNA. In the 23 unrelated patients belonging to group P, which had typical (frameshift, nonsense, missense) point or subtle CHM-causing mutations, we identified aberrant mRNAs that likely encoded very unstable proteins.[15,29] Indeed, the degradation of unstable proteins may in part explain the strong deficiency of REP1 usually detected in CHM patients' cells.[28] In contrast, the four unrelated probands belonging to group A had large genomic deletions that removed the whole *CHM* gene and/or regulatory sequences that drive its transcription. Therefore, the resulting ineffective gene expression leads to absent mRNA and consequently to total protein deficiency in these patients.

Comparing the two groups, we found a novel significant association between disease severity and *CHM/REP1* gene transcription, despite the fact that the REP1 protein is supposedly absent or strongly deficient in both groups of patients. In particular, according to the fitted regression models, the patients in group A showed a higher visual

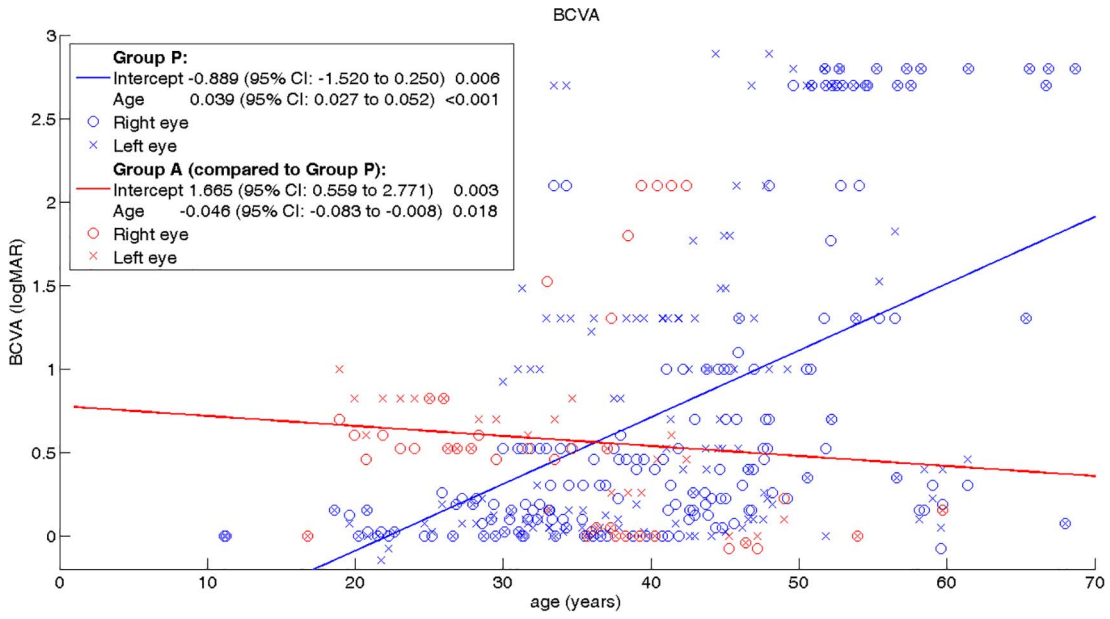

Figure 4. Regression models fit to compare BCVA according to *CHM/REP1* expression. For each model, the mean annual rate (95% confidence interval) with *P* value is reported.

function loss (in terms of reduced BCVA and constricted GVF) at younger ages (i.e., <30 years) when compared with the group P patients, followed by a slower progression of visual function loss. These findings could be explained by hypothesizing that, in the patients of group A, genomic deletions removed transcription factor–binding sites (i.e., promoter/enhancer) within the *CHM/REP1* gene that not only caused its silencing but also induced a spatial reorganization of chromatin. Such an aberrant chromatin structure could affect the expression of genes belonging to the same transcription network of *CHM/REP1* and, together with the total loss of REP1, contribute to perturb eye-specific gene expression programs, therefore explaining severe aspects of the phenotype in this group of patients when compared with group P.

The current study presents some limits, mainly related to its retrospective design and the relatively small sample size, particularly for RNA analysis. First, the follow-up length is not the same for all the patients. Second, the analysis of mRNA expression was not available in all of the families and consequently there are only a few independent patients who completely lacked the *CHM/REP1* transcript. Moreover, for these cases, there are limited data for those aged older than 55 years. Therefore, further prospective studies on a larger cohort of patients, eventually recruited from different centers, could be useful to confirm the findings of the current study.

In conclusion, our longitudinal analysis of the morphological and functional parameters in CHM patients shows a slow disease progression, particularly in the first decades of life. Moreover, our preliminary data show a more severe phenotype in patients with absent *CHM/REP1* transcription, particularly at a younger age, suggesting that further genotype–phenotype correlations in CHM patients could be explored by verifying that *CHM/REP1* transcription takes place regularly.

Acknowledgments

Supported by the Fondazione Telethon (funds to Francesca Simonelli) and by the Italian Ministry of Education, University and Research (Grants PON03PE_00060_2 and PON03PE_00060_7, Campania Bioscience to Franco Salvatore). The funding organizations had no role in the design or conduct of this research.

Disclosure: **V. Di Iorio**, None; **G. Esposito**, None; **F. De Falco**, None; **R. Boccia**, None; **T. Fioretti**, None; **R. Colucci**, None; **G. De Rosa**, None; **P. Melillo**, Sanofi (C), Shire (C); **F. Salvatore**, None; **F. Simonelli**, Sanofi (C), Spark Therapeutics (C); **F. Testa**, Sanofi (C), Shire (C)

References

1. MacDonald IM, Russell L, Chan CC. Choroideremia: new findings from ocular pathology and review of recent literature. *Surv Ophthalmol*. 2009;54:401–407.
2. Sankila EM, Tolvanen R, van den Hurk JA, Cremers FP, de la Chapelle A. Aberrant splicing of the CHM gene is a significant cause of choroideremia. *Nat Genet*. 1992;1:109–113.
3. Khan KN, Islam F, Moore AT, Michaelides M. Clinical and genetic features of choroideremia in childhood. *Ophthalmology*. 2016;123:2158–2165.
4. Seabra MC, Brown MS, Slaughter CA, Sudhof TC, Goldstein JL. Purification of component A of Rab geranylgeranyl transferase: possible identity with the choroideremia gene product. *Cell*. 1992;70:1049–1057.
5. Seabra MC, Ho YK, Anant JS. Deficient geranylgeranylation of Ram/Rab27 in choroideremia. *J Biol Chem*. 1995;270:24420–24427.
6. Freund PR, Sergeev YV, MacDonald IM. Analysis of a large choroideremia dataset does not suggest a preference for inclusion of certain genotypes in future trials of gene therapy. *Mol Genet Genomic Med*. 2016;4:344–358.
7. Roberts MF, Fishman GA, Roberts DK, et al. Retrospective, longitudinal, and cross sectional study of visual acuity impairment in choroideraemia. *Br J Ophthalmol*. 2002;86:658–662.
8. Coussa RG, Kim J, Traboulsi EI. Choroideremia: effect of age on visual acuity in patients and female carriers. *Ophthalmic Genet*. 2012;33:66–73.
9. Renner AB, Kellner U, Cropp E, et al. Choroideremia: variability of clinical and electrophysiological characteristics and first report of a negative electroretinogram. *Ophthalmology*. 2006;113:2066.
10. Barnard AR, Groppe M, MacLaren RE. Gene therapy for choroideremia using an adeno-associated viral (AAV) vector. *Cold Spring Harb Perspect Med*. 2015;5:a017293.
11. MacLaren RE, Groppe M, Barnard AR, et al. Retinal gene therapy in patients with choroideremia: initial findings from a phase 1/2 clinical trial. *Lancet*. 2014;383:1129–1137.
12. Krill A.E. *Hereditary Retinal and Choroidal Diseases*. Hagerstown, USA: Harper & Row; 1977
13. Iannaccone A, Kritchevsky SB, Ciccarelli ML, et al. Kinetics of visual field loss in Usher syndrome Type II. *Invest Ophthalmol Vis Sci*. 2004;45:784–792.
14. Marmor MF, Zrenner E. Standard for clinical electroretinography (1994 update). *Doc Ophthalmol*. 1995;89:199–210.
15. Esposito G, De Falco F, Tinto N, et al. Comprehensive mutation analysis (20 families) of the choroideremia gene reveals a missense variant that prevents the binding of REP1 with Rab geranylgeranyl transferase. *Hum Mutat*. 2011;32:1460–1469.
16. Zeger SL, Liang K-Y, Albert PS. Models for longitudinal data: a generalized estimating equation approach. *Biometrics*. 1988;1049–1060.
17. Fan Q, Teo YY, Saw SM. Application of advanced statistics in ophthalmology. *Invest Ophthalmol Vis Sci*. 2011;52:6059–6065.
18. Glynn RJ, Rosner B. Regression methods when the eye is the unit of analysis. *Ophthalmic Epidemiol*. 2012;19:159–165.
19. Rossi S, Orrico A, Melillo P, Testa F, Simonelli F, Della Corte M. Ocriplasmin use in a selected case with preserved visual acuity. *BMC Ophthalmol*. 2015;15:146.
20. Rossi S, Testa F, Melillo P, Orrico A, Della Corte M, Simonelli F. Functional improvement assessed by multifocal electroretinogram after Ocriplasmin treatment for vitreomacular traction. *BMC Ophthalmol*. 2016;16:110.
21. Testa F, Melillo P, Bonnet C, et al. Clinical presentation and disease course of Usher syndrome because of mutations in *Myo7a* or *Ush2a*. *Retina*. 2017;37:1581–1590.
22. Di Iorio V, Orrico A, Esposito G, et al. Association between genotype and disease progression in Italian Stargardt patients: a retrospective natural history study [published online ahead of print April 10, 2018]. *Retina*. doi:10.1097/IAE.0000000000002151.
23. Melillo P, Testa F, Rossi S, et al. En face spectral-domain optical coherence tomography for the monitoring of lesion area progression in Stargardt disease. *Invest Ophthalmol Vis Sci*. 2016;57:OCT247–OCT252.
24. Kong X, Strauss RW, Michaelides M, et al. Visual acuity loss and associated risk factors in the retrospective progression of Stargardt Disease Study (ProgStar Report No. 2). *Ophthalmology*. 2016;123:1887–1897.
25. Testa F, Melillo P, Di Iorio V, et al. Macular function and morphologic features in juvenile stargardt disease: longitudinal study. *Ophthalmology*. 2014;121:2399–2405.
26. World Health Organization. *International Statistical Classification of Diseases and Related Health Problems, 10th*

Revision. Geneva, Switzerland: World Health Organization; 2016.

27. Aleman TS, Han G, Serrano LW, et al. Natural history of the central structural abnormalities in choroideremia: a prospective cross-sectional study. *Ophthalmology*. 2017;124:359–373.
28. Furgoch MJ, Mewes-Ares J, Radziwon A, Macdonald IM. Molecular genetic diagnostic techniques in choroideremia. *Mol Vis*. 2014;20:535–544.
29. Beaufrere L, Tuffery S, Hamel C, et al. The protein truncation test (PTT) as a method of detection for choroideremia mutations. *Exp Eye Res*. 1997;65:849–854.

Investigative Ophthalmology & Visual Science